Effect of Epicardial Adipose Tissue–Derived Secretome on Atrial Fibrillation Vulnerability

Veronica Bergui[1], Chiara Celotto[1], Saman Golmaryami[2], Bettine van Willigen[3], Etel Silva Garcia[2], Elvio Alberto Heidenreich[4], Joris de Groot[3], Jose F. Rodriguez Matas[1]

[1] LaBS, Department of Chemistry, Materials and Chemical Engineering "Giulio Natta", Politecnico di Milano, Milan, Italy
[2] Instituto de Investigación e Innovación Biomédica de Cádiz (INiBICA), Grupo GADICOR, Hospital Universitario Puerta del Mar, Universidad de Cádiz, Cádiz, Spain
[3] Amsterdam UMC, Amsterdam, The Netherlands
[4]

Abstract

Epicardial adipose tissue (EAT) may promote atrial fibrillation (AF) through paracrine effects of its secretome (FS) on the adjacent myocardium. We calibrated an in silico description of FS-induced electrical remodeling and quantified its arrhythmogenic effects.

The Courtemanche–Ramirez–Nattel model, adapted to eight atrial regions, was modified to reproduce the action potential changes measured in myocytes exposed to EAT-conditioned medium: g_{K1} and g_{Na} reduced by 40%, g_{Kr} and g_{Ks} increased by 20%. Control and FS were simulated without and with AF-induced electrical remodeling (AFER). A 2 cm monodomain cable provided conduction velocity (CV), effective refractory period (ERP), wavelength (WL) and restitution; conductivity under FS was lowered to represent gap-junction remodeling.

FS depolarized the resting potential by 5.5 $\pm$ 0.5% and prolonged APD_{90} by 33.1 $\pm$ 4.8%. It reduced CV by 31.7% (no AFER) and 33.2% (AFER) and prolonged ERP by 61% and 64%, so that WL increased by $\approx$10%. Without AFER, FS lost 1:1 conduction below BCL = 400 ms, with 2:1 propagation; with AFER, restitution became nearly flat. FS therefore does not promote reentry through WL shortening; spatial heterogeneity and rate-dependent conduction failure are more likely mechanisms.

1. Introduction

Epicardial adipose tissue (EAT) lies in direct contact with the atrial myocardium, without an interposed fascial barrier. Its volume is associated with the incidence and persistence of atrial fibrillation (AF) and with grater recurrence after ablation than conventional indices of obesity [1, 2].

Two mechanisms have been proposed. The first is structural: adipose infiltration acts as a physical obstacle to propagation, causing activation delay, increased anisotropy and conduction block [1]. The second is paracrine: EAT secretes a mixture of adipokines, proinflammatory cytokines, free fatty acids and extracellular vesicle, called the fat secretome (FS). In the absence of a physical barrier, the FS diffuses into the adjacent myocardium and modifies cardiomyocyte electrophysiology [3, 4].

The second mechanism has been characterized experimentally only recently. Ernault et al. [5] exposed neonatal rat ventricular myocytes and tissue preparations to EAT-conditioned medium and reported a depolarized resting membrane potential (RMP), a prolonged action potential (AP), a reduced AP amplitude (APA) and upstroke velocity (UV), together with a reduction in conduction velocity (CV), and observed that these changes facilitated reentry. A comprehensive quantitative in silico description of secretome-induced electrical remodeling is still missing.

The present work addresses this gap by calibrating a human atrial cell model to reproduce the AP phenotype measured under FS exposure and by using a one-dimensional (1D) cable to quantify the effects of FS on CV, effective refractory period (ERP), wavelength (WL) and APD restitution, both in the absence and in the presence of AF-induced electrical remodeling (AFER).

2. Methods

2.1. Cellular model and calibration

The Courtemanche-Ramirez-Nattel (CRN) model of the human atrial myocyte [6] was used. Regional heterogeneity was reproduced by scaling the maximal conductances of eight regions as described in [7]: crista terminalis and

Bachmann's bundle (CT/BB), left and right atrium (LA, RA), left and right appendage (LAA, RAA), pulmonary veins (PV) and the mitral and tricuspid valve rings (MVR, TVR).

FS exposure was represented phenomenologically by modifying maximal ionic conductances to reproduce the AP markers measured in neonatal rat ventricular myocytes exposed to EAT-conditioned medium [5] (Table 1). g_{K1} and g_{Na} were reduced by 40%, while g_{Kr} and g_{Ks} were increased by 20%. The reduction of I_{K1} was introduced to depolarize the RMP and is consistent with the available experimental evidence [3, 5], and the reduction of g_{Na} follows the decrease in UV. The 20% increase of the delayed rectifiers has no direct experimental counterpart (proinflammatory cytokines rather inhibit I_{Kr} [3]) and was introduced to compensate for the APD prolongation produced by the other two changes, which would otherwise be too large.

AFER was reproduced by reducing I_{to}, I_{CaL} and I_{Kur} by 50%, 70% and 50%, respectively [8]. Four conditions were therefore considered: Control and FS, each without and with AFER.

Steady state was reached by pacing each single cell for 20 min at a basic cycle length (BCL) of 800 ms and, independently, for 25 min at BCL = 1000 ms. RMP, APD at 20%, 50% and 90% repolarization, APA and maximum UV (dV/dt_{max}) were measured on the last beat and expressed as the percentage change with respect to the control cell of the same region.

2.2. One-dimensional tissue model

Monodomain propagation was solved with ELVIRA [9] on a 2-cm cable discretized with 100 linear elements (Δx = 200 μm, 101 nodes). All nodes were initialized at the corresponding single-cell steady state (CNR, LA variant). Stimuli of 2 ms duration and 380 pA/pF amplitude were applied at the proximal end.

Tissue conductivity was calibrated separately for the two substrates: 0.0038 S/m for Control and 0.0028 S/m for FS. The reduction was introduced to represent the remodeling of gap junctions and the associated decrease in intercellular coupling reported for EAT-exposed myocardium [1, 5]. It was calibrated to reproduce the experimentally measured 33.5% reduction in CV [5].

CV was computed from the activation times at x = 0.5 cm and x = 1.5 cm on the last two beats of a train of 100 S1 stimuli delivered at BCL = 800 ms. ERP was then measured with an S1-S2 protocol by scanning the coupling interval from 700 to 100 ms and refining the transition with 1-ms resolution. ERP was defined as the longest coupling interval for which S2 failed to propagate to at least one of the five equispaced observation nodes. WL was estimated as the product CV $\times$ ERP. Dynamic restitution was assessed by applying trains of 100 stimuli at decreasing BCL (1000, 800, 700, 600, 500, 450, 400, 350, 300, 275 and 250 ms) and computing the mean and standard deviation of APD_{50}, APD_{80} and APD_{90} over the last ten beats of each train.

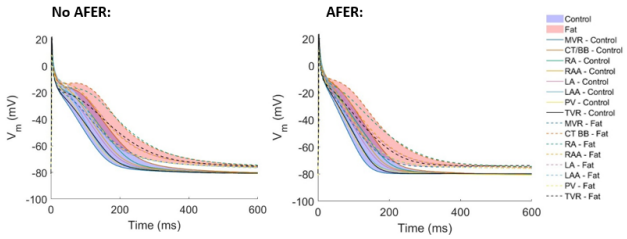

Figure 1. Action potentials for the eight atrial regions in Control and FS conditions, without (left) and with (right) AF-induced electrical remodeling (AFER). Solid and dashed curves denote Control and FS, respectively; colors identify the different atrial regions.

3. Results

3.1. Cellular level

Table 1 reports the percentage changes induced by FS, averaged over the eight atrial regions, during pacing at BCL = 800 ms. The reduction in APA was close to the experimental target in all regions, whereas the RMP shift and the reduction in maximum UV were approximately half of the corresponding experimental changes. APD_{90} was prolonged beyond the target value of $+20\%$. APD_{50} and APD_{20}, for which no change was reported experimentally, increased by $39.2 \pm 8.1\%$ and $45.7 \pm 7.5\%$, respectively.

Regional variability was small for RMP, APA and dV/dt_{max} (standard deviation below 1.1 percentage points) and larger for APD: the prolongation of APD_{90} ranged from $+26.8\%$ in the LAA to $+41.4\%$ in the TVR. Pacing at BCL = 1000 ms produced differences below three percentage points for all markers and is therefore not reported. Representative action potentials for the eight atrial regions are shown in Figure 1. FS induces a depolarization of the RMP and prolongs repolarization in all regions, with the largest differences emerging during the later phases of the action potential. The regional differences in action potential morphology are maintained in the presence of AFER.

AFER did not change the direction of the FS-induced effects. It slightly increased the changes in RMP, APA and dV/dt_{max} and reduced both the magnitude and regional dispersion of APD prolongation.

Table 1. Percentage change of the AP markers in FS with respect to the corresponding Control, given as mean $\pm$ SD over the eight atrial regions (BCL = 800 ms), and experimental targets [5].

Marker	Target [5]	FS	FS + AFER
RMP	$+10\%$	$+5.5 \pm 0.5$	$+6.5 \pm 0.8$
APD_{90}	$+20\%$	$+33.1 \pm 4.8$	$+29.6 \pm 4.2$
APD_{50}	~ 0	$+39.2 \pm 8.1$	$+32.9 \pm 4.8$
APD_{20}	~ 0	$+45.7 \pm 7.5$	$+43.6 \pm 7.0$
APA	-15%	-14.9 ± 0.5	-16.1 ± 1.0
$dV/dt_{\max}$	-67%	-35.5 ± 0.9	-37.8 ± 2.1

Table 2. Conduction velocity, effective refractory period and wavelength (WL = CV $\times$ ERP) measured in the 1D cable.

Case	CV (cm/s)	ERP (ms)	WL (cm)
Control	90.9	226	20.5
Control + AFER	93.5	191	17.9
FS	62.1	363	22.5
FS + AFER	62.5	313	19.6

3.2. Tissue level

CV, ERP and WL for the four conditions are reported in Table 2. With the ionic changes alone and control conductivity, CV decreased by 14.8% without AFER and 17.8% with AFER. Including the reduction in tissue conductivity increased the total decrease to 31.7% and 33.2%, respectively, close to the experimental reduction of 33.5% [5].

FS prolonged ERP by 61% without AFER and by 64% with AFER. AFER shortened ERP by 35 ms in Control and by 50 ms in FS, while changing CV only slightly ($+2.9\%$ and $+0.6\%$, respectively). As a result, WL was approximately 10% longer under FS than in the corresponding control condition. The shortest WL was obtained with AFER in the absence of FS.

The dynamic restitution curves are shown in Figure 2. In both Control conditions and in FS without AFER, APD increased monotonically with BCL. In FS without AFER, 1:1 propagation was lost below BCL = 400 ms. The cable propagated one impulse for every two stimuli, and restitution curves were therefore not computed at lower BCL values. In FS with AFER, 1:1 propagation was maintained down to BCL = 250 ms, but APD varied little with BCL, indicating reduced rate adaptation.

4. Discussion

The calibration reproduces the experimental AP phenotype only partially. APA is reproduced closely, whereas the RMP shift and the reduction in $dV/dt_{\max}$ reach approximately half of the measured changes. APD_{20} and APD_{50}, for which no experimental change was reported,are indeed prolonged. A possible explanation is the mismatch between the experimental source of the target APs and the model used for calibration: APs from neonatal rat ventricular myocytes are essentially triangular, whereas the CRN model reproduces the spike-and-dome morphology characteristic of the human atrial AP. In the CRN formulation, any combination of conductance changes that prolongs APD_{90} to the required extent also acts on the plateau, so the two constraints cannot be satisfied simultaneously by a small set of scaling factors.

The increase in g_{Kr} and g_{Ks} should be interpreted with the same caution. It is not consistent with the inhibition of hERG reported for IL-6 and other cytokines contained in the secretome [3], and should be regarded as a correction that keeps repolarization within the measured range rather than as a mechanistic hypothesis.

At the tissue level, the results show that the experimental CV reduction cannot be reproduced by ionic remodeling alone. The ionic changes produced a 14.8% reduction in CV without AFER, compared with 31.7% after the additional reduction in tissue conductivity. This is consistent with the reported remodeling of gap junctions in EAT-exposed myocardium [1, 5] and indicates that both cellular ionic remodeling and reduced intercellular coupling contribute to the observed slowing of conduction.

The effects of FS and AFER on refractoriness are not additive. The two act in opposite directions: FS prolongs ERP, whereas AFER shortens it. Because FS slows conduction and lengthens ERP simultaneously, WL is longer under FS than in the corresponding control condition. Thus, the wavelength criterion alone does not predict an increased vulnerability to reentry under FS. Since experiments report the opposite [4, 5], other mechanisms have to be considered. Two mechanisms are suggested by the present results. The first is spatial heterogeneity. The nonuniform distribution of EAT and the spatial penetration of its effects can generate regions with different electrophysiological properties, creating conditions favorable to conduction block and reentry. The second is rate-dependent conduction failure. FS without AFER lost 1:1 propagation below BCL = 400 ms and therefore failed to sustain higher stimulation rates. In a spatially heterogeneous substrate, such rate-dependent conduction failure may contribute to wave break and reentry. The nearly flat restitution obtained with FS and AFER further indicates reduced rate adaptation.

The study has some limitations. The calibration targets are derived from animal data and from a limited set of AP markers; calcium-handling alterations reported for EAT exposure [3] were not included; and interpatient variability in secretome composition is not represented. Extension to anatomically detailed biatrial models with patient-specific fat distributions is required to assess these mechanisms in a spatially resolved substrate.

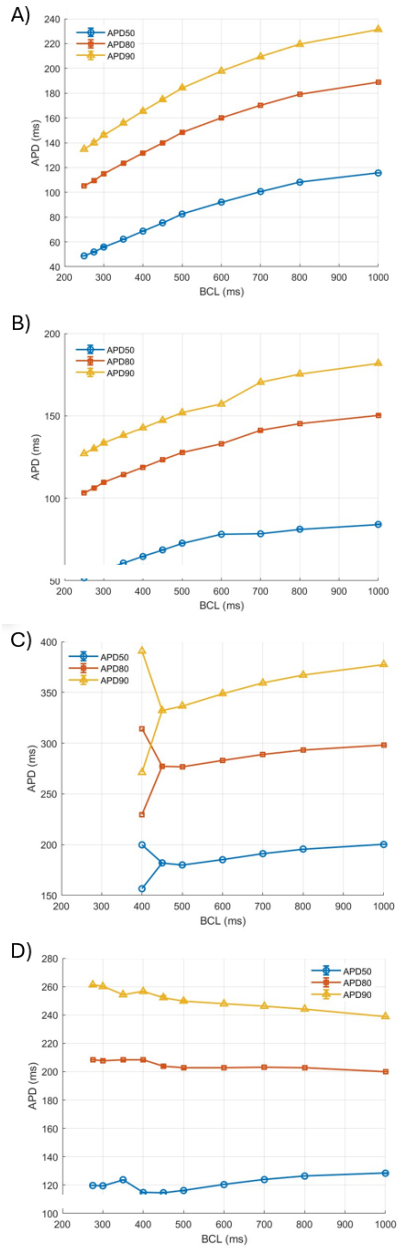

Figure 2. Dynamic restitution of APD_{50}, APD_{80} and APD_{90} (mean $\pm$ SD over the last ten beats of each train): (A) Control, (B) Control + AFER, (C) FS, (D) FS + AFER.

5. Conclusions

A CRN-based description of FS-induced electrophysiological remodeling was calibrated at the cellular level and characterized in a 1D cable. FS shifted the resting potential toward less negative values, prolonged APD, reduced APA and $dV/dt_{\max}$, slowed conduction by approximately one third, and prolonged ERP. The reduction in CV required both cellular ionic remodeling and reduced tissue conductivity. Because WL was longer under FS than in the corresponding control condition, the effect of FS on reentry is likely explained by spatial heterogeneity and rate-dependent conduction failure and should therefore be investigated using spatially resolved models.

Acknowledgments

Supported by the ERA4Health Partnership, the European Union through Horizon Europe under Grant Agreement 101095426, ERA4HEALTH CVD-124 PERSUADE, and the Spanish Ministry of Science under Grant PCI2024-153442.

References

[1] Ernault AC, Meijborg VMF, Coronel R. Modulation of cardiac arrhythmogenesis by epicardial adipose tissue: JACC state-of-the-art review. *J Am Coll Cardiol* 2021;78:1730–1745.

[2] Wong CX, Sun MT, Odutayo A, et al. Associations of epicardial, abdominal, and overall adiposity with atrial fibrillation. *Circ Arrhythm Electrophysiol* 2016;9:e004378.

[3] Patel KHK, Hwang T, Se Liebers C, Ng FS. Epicardial adipose tissue as a mediator of cardiac arrhythmias. *Am J Physiol Heart Circ Physiol* 2022;322:H129–H144.

[4] Shaihov-Teper O, Ram E, Ballan N, et al. Extracellular vesicles from epicardial fat facilitate atrial fibrillation. *Circulation* 2021;143:2475–2493.

[5] Ernault AC, Verkerk AO, Bayer JD, et al. Secretome of atrial epicardial adipose tissue facilitates reentrant arrhythmias by myocardial remodeling. *Heart Rhythm* 2022;19:1461–1470.

[6] Courtemanche M, Ramirez RJ, Nattel S. Ionic mechanisms underlying human atrial action potential properties: insights from a mathematical model. *Am J Physiol* 1998;275:H301–H321.

[7] Ferrer A, Sebastián R, Sánchez-Quintana D, et al. Detailed anatomical and electrophysiological models of human atria and torso for the simulation of atrial activation. *PLoS One* 2015;10:e0141573.

[8] Courtemanche M, Ramirez RJ, Nattel S. Ionic targets for drug therapy and atrial fibrillation-induced electrical remodeling: insights from a mathematical model. *Cardiovasc Res* 1999;42:477–489.

[9] Heidenreich EA, Ferrero JM, Doblaré M, Rodríguez JF. Adaptive macro finite elements for the numerical solution of monodomain equations in cardiac electrophysiology. *Ann Biomed Eng* 2010;38:2331–2345.

Address for correspondence:

Jose F Rodriguez Matas

Politecnico di Milano, Piazza Leonardo da Vinci 32, 20133 Milan, Italy

josefelix.rodriguezmatas@polimi.it